0026-895X/06/6906-1849–1860$20.00
MOLECULAR PHARMACOLOGY
Copyright © 2006 The American Society for Pharmacology and Experimental Therapeutics
Mol Pharmacol 69:1849–1860, 2006

Vol. 69, No. 6
22772/3116245
Printed in U.S.A.

Determination of Binding Site Residues Responsible for the Subunit Selectivity of Novel Marine-Derived Compounds on Kainate Receptors

James M. Sanders, Olli T. Pentikäinen, Luca Settimo, Ulla Pentikäinen, Muneo Shoji, Makoto Sasaki, Ryuichi Sakai, Mark S. Johnson, and Geoffrey T. Swanson

Department of Pharmacology and Toxicology, University of Texas Medical Branch, Galveston, Texas (J.M.S., G.T.S.); Department of Biochemistry and Pharmacy, Åbo Akademi University, Turku, Finland (O.T.P., L.S., M.S.J.); Department of Pharmacology (O.T.P.) and the School of Chemistry (U.P.), University of Bristol, Bristol, United Kingdom; Laboratory of Biostructural Chemistry, Graduate School of Life Sciences, Tohoku University, Sendai, Japan (M.Sh., M.Sa); and School of Fisheries Sciences, Kitasato University, Iwate, Japan (R.S.)

Received January 19, 2006; accepted March 14, 2006

ABSTRACT

Dysiherbaine (DH) and related molecules are high-affinity, subunit-selective kainate receptor (KAR) ligands originally isolated from a marine sponge. To elucidate why DH, an agonist, and MSVIII-19, a competitive antagonist, bind selectively to glutamate receptor (GluR) 5 but not to the KA2 KAR subunit, we used molecular dynamics simulations to generate binding models that were tested experimentally in radioligand binding and electrophysiological assays. Three candidate sites, Val685, Leu735, and Ser741 in GluR5, corresponding to Ile669, Phe719, and Met725 in KA2, were predicted to underlie the distinct binding profiles of the marine toxins. Single or multiple reciprocal mutations introduced into the receptor subunits produced a variety of effects on binding affinity. Most notably, mutation of Met725 to serine in KA2 increased the affinity of DH by 350-fold; in contrast, mutation of one or more of the residues in GluR5 did not markedly alter DH binding. MSVIII-19 affinity for the KA2 subunit was significantly increased in multiple site mutants, and reciprocal mutations in the GluR5 subunit produced substantial (700-fold) reductions in MSVIII-19 affinity. Physiological characterization of the double- and triple-mutant subunits demonstrated altered functional behavior consistent with the changes in binding affinity. The results provide experimental support for the importance of these three ligand binding domain (LBD) residues and suggest steric hindrance in the KA2 subunit LBD is largely responsible for the very low affinity for the two compounds. In this study, we identified the molecular basis for subunit selectivity of these marine-derived molecules on KARs, which could facilitate the rational design of selective ligands with distinct pharmacological profiles.

Ionotropic glutamate receptors (iGluRs) comprise the primary mechanism for excitatory neurotransmission in the brain and contribute to numerous physiological and pathophysiological processes (Dingledine et al., 1999). IGluRs are subdivided into NMDA, AMPA, and kainate receptors (KARs) based on pharmacology and sequence homology (Hollmann and Heinemann, 1994). Selective pharmacological agents have been critical aids in determining the roles of distinct iGluRs in the CNS, but elucidation of the role of KARs has been hampered by a relative paucity of subunit-selective antagonists (Kew and Kemp, 2005). Compounds that act as competitive and noncompetitive GluR5 receptor antagonists have become commercially available (Christensen et al., 2004; More et al., 2004), but no equivalent set of antagonists exist that are specific for GluR6-containing receptors. Compounds that selectively work on kainate receptors hold promise for the treatment of pathophysiological states such as migraine, pain, and epilepsy (Sang et al., 1998, 2004; Gilron et al., 2000; Barton et al., 2003).

We have characterized the activity of dysiherbaine (DH), a naturally occurring amino acid isolated from the marine

This study was supported by Academy of Finland, Technology Development Center of Finland, Sigrid Jusélius Foundation, National Graduate School in Informational and Structural Biology (L.S., O.T.P., U.P., and M.S.J.) and the National Institute for Neurological Diseases and Stroke (J.S., G.T.S.).
Article, publication date, and citation information can be found at http://molpharm.aspetjournals.org.
doi:10.1124/mol.106.022772.

ABBREVIATIONS: IGluR, ionotropic glutamate receptor; NMDA, *N*-methyl-D-aspartate; AMPA, (*S*)-α-amino-3-hydroxy-5-methyl-4-isoxazolepropionic acid; KAR, kainate receptor; DH, dysiherbaine; LBD, ligand binding domain; GLU, L-glutamate; LAO-BP, lysine-arginine-ornithine binding protein; MD, molecular dynamics; ATPA, (*R*,*S*)-2-amino-3-(3-hydroxy-5-*tert*-butylisoxazol-4-yl)propanoic acid; MSVIII-19, (2*R*,3*aR*,7*aR*)-2-[(2*S*)-2-amino-2-carboxy-ethyl]-hexahydro-furo[3,2-*b*]pyran-2-carboxylic acid.

sponge *Dysidea herbacea*, and MSVIII-19, a synthetic analog of DH, on ionotropic and metabotropic glutamate receptors (Sakai et al., 2001; Sanders et al., 2005). The structures of the two compounds differ at the C8 and C9 positions on the integral ring structure; DH contains methylamine and hydroxyl groups, respectively, whereas MSVIII-19 lacks functional groups at these positions (Sakai et al., 1997, 1999) (Fig. 1A). DH potently activates kainate receptors (Sakai et al., 2001), whereas MSVIII-19 is a competitive antagonist (Sanders et al., 2005). Both compounds show a high degree of subunit selectivity within the KAR family. In particular, DH binds to GluR5 and GluR6 subunits with affinity 4 orders of magnitude higher than for KA2 subunits (Swanson et al., 2002). MSVIII-19, in contrast, is a selective, competitive antagonist for GluR5-containing kainate receptors with no detectable affinity for GluR6 or KA2 subunits (Sanders et al., 2005). Together, these studies have shown the critical role that the molecular constituents C8 and C9 play in determining the pharmacological profile of the molecule.

It is important to understand the interactions that occur in the LBD to understand the basis for the selective binding of ligands. Ligand binding to glutamate receptors occurs at two distinct parts within each subunit; the S1 domain is contained in the N-terminal domain of the receptor and the S2 domain forms part of the loop between the second and third transmembrane domains (Stern-Bach et al., 1994). Binding of ligands to AMPA receptor LBDs results in variable degrees of domain closure that correlates with a compounds ability to act as a full agonist, partial agonist, or antagonist (Armstrong and Gouaux, 2000; Hogner et al., 2003; Jin et al., 2003). Multiple crystal structures have been determined for GluR5 in complex with glutamate (Naur et al., 2005), GluR6 in complex with domoic acid (Nanao et al., 2005), and GluR5 and GluR6 subunits in complex with glutamate, kainate, quisqualate, and (2*S*,4*R*)-4-methylglutamate (Mayer, 2005), but no crystal structures exist for DH or MSVIII-19 bound to KARs.

We generated models of kainate receptor LBDs docked with DH and MSVIII-19 to visualize interactions that might be responsible for the binding and subunit selectivity of these compounds. These models predicted that three amino acid residues account for the difference in DH affinity between subunits (Sanders et al., 2005). To understand further the molecular environment of ligand interactions with KAR subunits, we used homology models in tandem with molecular dynamics (Pentikäinen et al., 2006) of DH and MSVIII-19 docked within the wild-type and mutated LBDs. To test the model predictions, we made site-directed mutants and tested them using radioligand binding and whole-cell, patch-clamp recordings. Our results provide insight into the interactions critical for the subunit selectivity of the marine-derived compounds and largely validate our previous model and that generated by molecular dynamics simulations. Furthermore, these results will be useful for predicting how the DH structure could be modified to produce KAR ligands with unique selectivity profiles.

Materials and Methods

Molecular Biology. GluR5–2a, myc-KA2, and GFP-GluR5–2b cDNAs were kindly supplied by Peter Seeburg (University of Heidelberg, Heidelberg, Germany) and John Marshall (Brown University, Providence, RI). KA2(I669V), KA2(F719L), KA2(M725S), KA2(I669-V/M725S), KA2(I669V/F719L/M725S), GluR5(V685I), GluR5(L-735F), GluR5(S741M), GluR5(V685I/S741M), and GluR5(V685I/L-735F/S741M) cDNAs were made using the QuikChange site mutagenesis protocol (Stratagene, La Jolla, CA). DNA sequencing was performed on all mutations.

Electrophysiology. Human embryonic kidney 293 cells were transfected with receptor cDNAs (0.05–0.3 μg) in combination with enhanced green fluorescent protein cDNA for the visualization of transfected cells. A ratio of 1:3 GluR5(R) to KA2 cDNA was used for expression of heteromeric KAR receptors. Patch-clamp recordings from transfected cells were made 24 to 72 h later. The internal solution contained 110 mM CsF, 30 mM CsCl, 4 mM NaCl, 0.5 mM $CaCl_2$, 10 mM HEPES, and 5 mM EGTA (adjusted to pH 7.3 with CsOH). The external bath solution was composed of 150 mM NaCl, 2.8 mM KCl, 2 mM $CaCl_2$, 1.0 mM $MgCl_2$, 10 mM HEPES, and 10 mM glucose (pH adjusted to 7.3 with NaOH). Patch electrodes were pulled from thick-walled borosilicate glass (Warner Instruments, Hamden, CT) with a final resistance of 1.5 to 2.5 MΩ after fire polishing. Fast application of drugs was achieved through a three-barrel glass tube mounted to a piezobimorph, as described previously (Sanders et al., 2005). In brief, cells were lifted from coverslips to provide laminar flow across the cells. Fast application of drugs was achieved by applying transistor-transistor logic pulses controlled by pClamp9 (Axon Instruments, Union City, CA). Glutamate applications occurred every 20 s during control periods and after application of DH. Whole-cell, patch clamp recordings were performed with an Axopatch 200B amplifier (Axon Instruments). The holding potential for all patch-clamp recordings was −70 mV. Data were acquired and analyzed using pClamp9 software (Axon Instruments), Origin 6.0 (OriginLab Corp., Northhampton, MA), and Prism 4 (GraphPad Software Inc., San Diego, CA).

Radioligand Binding. Membrane preparations from COS-7 cells were prepared as described previously (Sanders et al., 2005). Unlabeled DH and MSVIII-19 were used to displace the radioligand [^{3}H]kainate (7–25 nM; PerkinElmer Life and Analytical Sciences, Boston, MA), from KAR subunits in COS-7 membranes. Nonspecific binding was measured in the presence of 1 mM glutamate. Membranes were incubated at 4°C for 1 h and harvested by rapid filtration through Whatman GF/C membranes. After addition of scintillation fluid, membranes were incubated at room temperature for 1 h before quantitation on a scintillation counter (LS5000 TD; Beckman Coulter, Fullerton, CA). Data were graphed and fitted with a one-site competition curve using Prism 4 (GraphPad Software). Saturation experiments were performed as above with varying concentrations of [^{3}H]kainate (PerkinElmer Life and Analytical Sciences). Saturation curves were plotted and fit with a one-site binding (hyperbola) using Prism 4 (GraphPad Software).

Protein Models. Protein crystal structures were downloaded from the Protein Data Bank. The crystal structure of the ligand binding domain of GluR5 in complex with the natural ligand L-glutamate (GLU; Protein Data Bank code 1ycj) (Naur et al., 2005) was used for studies of ligand binding to the GluR5 subunit. For homology modeling of the KA2 LBD, the model was based on sequence alignment of GluR2, GluR5, and KA2 subunits made using Malign in the Bodil Modeling Environment (Lehtonen et al., 2004) using a structure-based sequence comparison matrix with gap formation penalty of 40 (Johnson and Overington, 1993), as described previously (Sanders et al., 2005). The program Homodge in Bodil was used to construct a three-dimensional model structure for the KA2 LBD by using X-ray structures of GluR2-GLU, GluR5-GLU, and lysine-arginine-ornithine binding protein (LAO-BP) as templates. The crystal structures of GluR2 and GluR5 LBDs bound with the natural ligand L-glutamate were used as a template to build a structural model of the KA2 LBD, except that the crystal structure of LAO-BP (Oh et al., 1994) was used as a structural template for the area Ala498–Ala499. This was done because the LAO-BP shows different main chain angles near this position, in contrast to all

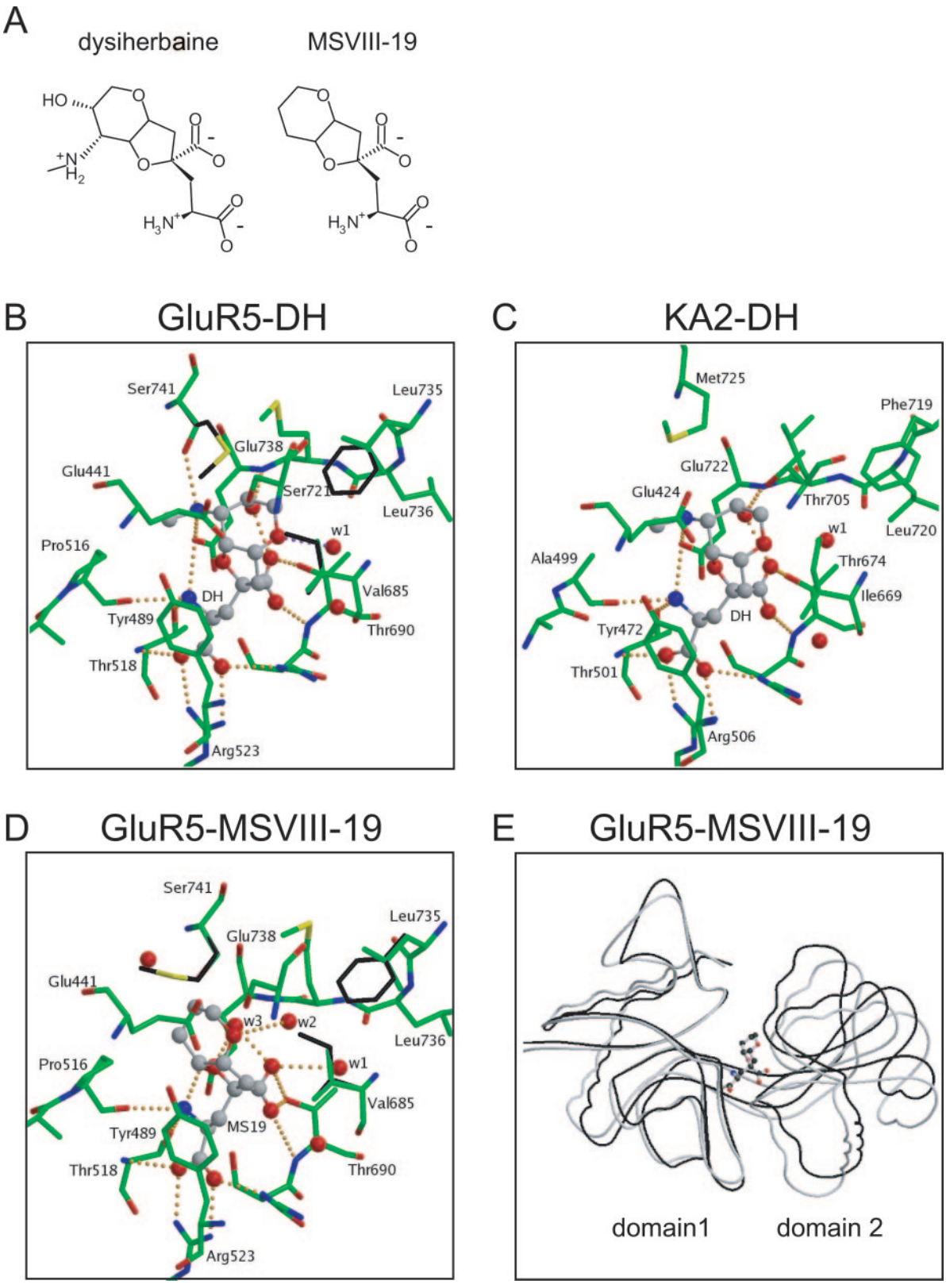

Fig. 1. Molecular dynamic simulations of DH and MSVIII-19 binding to GluR5 and KA2 LBDs. A, chemical structures of dysiherbaine (DH) and MSVIII-19. B, model of DH bound to GluR5. C, model of DH bound to the KA2 subunit. D, model of MSVIII-19 bound to GluR5 subunit. Ligands are shown as ball-and-stick models with gray carbon atoms; GluR5 and KA2 subunits are shown with sticks with green carbon atoms; and water molecules are represented as red spheres (w1 or w2). The three KA2 residues exchanged reciprocally in this study are shown in black superimposed on the GluR5 structure. Orange dashed lines represent hydrogen bonding between the ligand and receptor, ligand and water molecules, and within the ligand itself. MSVIII-19 induces a more open conformation than seen for DH. E, ribbon diagram represents a comparison of domain closure between the full agonist DH (black coil) and the antagonist MSVIII-19 (gray coil). Ligand shown is MSVIII-19.

published iGluR X-ray structures. GluR1–7 subunits have the sequence Ala-Pro in this area, the NR2A subunit has Gly-Ser, and the LAO-BP contains the sequence Ser69-Ser70; the latter is most similar to the KA2 subunit. Use of the LAO-BP template produces a structural model of KA2 LBD in which Tyr472 forms a hydrogen bond with the main chain oxygen of Ala499 (see Fig. 1C, hydrogen bond not shown), instead of the side-chain carboxylate of Glu424 that is seen in the GluR2, GluR5, and GluR6 crystal structures. However, this modification does not alter significantly the position of phenyl ring of Tyr472. During the model building, the side-chain conformations of all identical residues remained fixed, and the corresponding torsion angles of similar residues in the alignment were maintained. Because Homodge does not perform any optimization of the protein structure, the intramolecular atom-atom clashes were removed by using the amino acid side-chain rotamer library (Lovell et al., 2000) incorporated within Bodil. For ligand docking, the hydrogen atoms for the GluR5 structure and KA2 model were added using the program Reduce (Word et al., 1999).

Ligand Structures and Docking. Ligand structures were optimized quantum mechanically with Gaussian03 (Frisch et al., 2004) at the HF/6–31+G* level in a continuum solvent model (water, using the PCM model of Gaussian03). Trajectories obtained from the molecular dynamics (MD) simulations were analyzed with the ptraj module of AMBER 8.0. Optimized ligands were docked flexibly into the GluR5 and KA2 receptors with Gold 2.2 (Jones et al., 1995, 1997). The search area was limited to a 15-Å radius sphere centered at the C^{δ}-atom of Glu738 in GluR5 and Glu722 in KA2.

Molecular Dynamics. The ligand-receptor complex structures obtained from the docking studies were used as starting structures for the MD simulations. Water molecules seen in the X-ray structure of the GluR5 receptor with glutamate bound were included in the starting structures. However, because DH and MSVIII-19 are bulkier ligands than glutamate, which is seen in the crystal structure, those water molecules that were closer than 1.4 Å from any atom of protein-ligand complex were excluded. Because the water molecules were not present in the docking simulation, the exclusion distance was set lower than the van der Waals distance. This option guaranteed that all cavities were filled with solvent molecules. The force field parameters for the protein were taken from the parm99 parameter set (Wang et al., 2004) of AMBER 8.0 (Case et al., 2005) and for the ligands from the gaff parameter set (Wang et al., 2004). The electrostatic potentials of the optimized ligands were obtained from *ab initio* quantum mechanical single point energy calculations (HF/6–31+G* with Gaussian03) (Frisch et al., 2004) performed for the structure obtained from the solution optimization. Atom-centered point charges for corresponding atoms were generated from the electrostatic potential using the restrained electrostatic potential method (Bayly et al., 1993; Cornell et al., 1993; Cieplak et al., 1995). The charges of chemically equivalent atoms were set to equal values.

The ligand-receptor complexes were solvated with a box of transferable intermolecular potential three-point waters extending 13 Å in all dimensions around the solute using the LEAP (Schafmeister et al., 1995) module of AMBER 8.0. The system was then neutralized by adding the appropriate number of sodium or chloride counter ions.

Energy minimizations and molecular dynamics simulations were performed using the PMEMD module of Amber 8. Equilibration was performed using the following procedure. In the first step, the hydrogen atoms in the system were minimized using the steepest decent algorithm (20 steps) and then with the conjugate gradient method (6980 steps) keeping the rest of the system fixed, followed by a similar relaxation of the water molecules. At the third step, a 30-ps MD simulation for water molecules was performed, the system was heated from an initial temperature of 100 K to 300 K in 30 ps, and thereafter the temperature was maintained at 300 K. After relaxation of the water molecules, the system was energy-minimized for 8000 steps, where the protein main chain was kept rigid for the first 3000 steps. Unrestrained molecular dynamic simulations of the whole system were started by heating up the whole system as was done in the equilibration MD simulation of the water molecules. After that, a 75-ps simulation at constant volume was done. Finally, the production simulations of 2.25 ns at constant temperature (300 K) and pressure (1 atm) was performed. All simulations were run using a 1.5-fs step time. A cutoff of 8.0 Å was used for van der Waals interactions, and the long-range electrostatic interactions were treated using the particle mesh Ewald summation method (Darden et al., 1993; Essmann et al., 1995; Sagui and Darden, 1999) with a charge grid spacing of ~1.0 Å. Bonds containing hydrogen atoms were constrained using the SHAKE algorithm (Ryckaert et al., 1977). Figures containing structural models were prepared using Bodil as described previously (Sanders et al., 2005), Molscript (Kraulis, 1991), and Raster3D (Merritt and Bacon, 1997).

Materials. DH was isolated as described previously (Sakai et al., 1997). MSVIII-19 was synthesized as described previously (Sasaki et al., 1999).

Results

Modeling the Binding of DH and MSVIII-19 to GluR5 and KA2 Subunits. Our objective in this study was to understand the nature of the interactions between DH and MSVIII-19 and the LBDs of KAR subunits, which would provide insight into the pharmacological specificities of these molecules. We have generated models for DH bound to the GluR5 and KA2 subunit LBDs by homology with the resolved GluR2-ATPA structure (Sanders et al., 2005). Likewise, the resolved structures of GluR5 and GluR6 KAR subunit LBDs were reported in complex with a number of agonists (Mayer, 2005; Nanao et al., 2005; Naur et al., 2005). We used this information and molecular dynamics simulations to refine our homology models, yielding testable hypotheses regarding the interactions between the marine-derived compounds and the GluR5 and KA2 LBDs (Fig. 1).

Docking of DH to the GluR5 LBD results in a conformation in which all polar atoms of the ligand interact with components of the binding cavity. In addition, the MD simulations yielded a similar, highly stable conformation with only slight adjustments around the ligand (Fig. 1B). The binding mode of the polar elements of the glutamate backbone is very similar to that observed for the GluR5-GLU structure (Mayer, 2005; Naur et al., 2005). The high affinity of DH for GluR5 is probably achieved through interactions between other polar groups in the DH molecule and elements of both domains 1 and 2 of the LBD structure. The amine in the C8 functional group donates hydrogen bonds to the side-chain carboxylate group of Glu738 and side-chain hydroxyl group of Ser741, the C9 hydroxyl group accepts a hydrogen bond from the main chain amino group of Glu738 and donates an intramolecular hydrogen bond to the γ-carboxylate group in DH, and the oxygen in the tetrahydropyran ring accepts a hydrogen bond from a water molecule (Fig. 1B, w1) that is stabilized by the main chain amino group of Val685 and carbonyl group of Leu736. In conclusion, our model predicts 12 hydrogen bonds between DH and the GluR5 LBD, one hydrogen bond between DH and a water molecule, and one intramolecular hydrogen bond in DH, thus accounting for the high affinity binding.

We also modeled DH binding to the KA2 subunit using the new KAR structures as templates to refine our previous proposal that the markedly lower affinity of DH for the KA2 subunit resulted from steric hindrance in the LBD introduced by a limited set of residues distinct from those in the

GluR5 LBD (Sanders et al., 2005). During the molecular dynamics simulation, the LBD of KA2 adjusted its conformation (relative to the composite GluR2/GluR5/LAO-BP template) to accommodate the bulkier Ile669, Phe719, and Met725 residues. The Ile669 side chain forces Phe719 further away from the DH binding site, which creates a greater distance between the critical binding domains formed by Ser673-Thr674 and Glu722 than is observed in the parent LBD structure. This adjustment produces less favorable conditions for bonding to the γ-carboxylate and 9-hydroxyl moieties on DH (Fig. 1C). In addition, Ile669 affects the position of Thr705, forcing it further away from the ligand and into a close packing conformation with water molecule w1 that could hinder the formation of an H-bond between the latter and DH. The presence of Ile669 occludes interactions between the two lobes of the LBD, which therefore adopts a more "open" conformation than that modeled for GluR5 with DH. The interaction with the ligand is further destabilized by the presence of Met725, which is unable to accept the hydrogen bonds from the C8 methylamine group that occur with Ser741 in the GluR5 LBD.

The chemical structure of MSVIII-19 differs from DH in that MSVIII-19 lacks substituents at the C8 and C9 positions (Fig. 1A), resulting in a significant reduction in the affinity of the molecule for GluR5 and other KAR subunits (Sanders et al., 2005). The absence of these moieties in the docked MSVIII-19-GluR5 structure creates spaces that were filled with water molecules. MD simulation suggested that the interactions between the α- and γ-carboxyl groups of MSVIII-19 and residues in the binding cavity were similar compared with DH (Fig. 1D). However, the overall conformation is distinct because the removal of the two polar substituents on the ring-system from MSVIII-19 causes packing of the ring system against the S1 hydrophobic face formed by residues Glu441, Tyr489 and, more distantly, Pro516 (Fig. 1D). A water molecule substitutes for the C9 hydroxyl group in DH (Fig. 1D, w3) and accepts a hydrogen bond from the main-chain amino group of Glu738 and stabilizes the ligand position by donating two hydrogen bonds to the γ-carboxylate group and oxygen atom in the tetrahydrofuran ring of the ligand. Because of these differences, the two lobes of the binding domain are more separated with MSVIII-19 than with DH (or with other agonists in the resolved structures), consistent with the antagonist activity of MSVIII-19 (Fig. 1E).

We also attempted to use MD simulations to model MSVIII-19 interactions with the KA2 LBD, which previous docking efforts were unable to resolve satisfactorily. This simulation was initiated with the MSVIII-19—GluR5 LBD conformation arrived at previously. The sequence differences in the LBDs resulted in adjustments around the ligand; the KA2 receptor structure remained fairly stable at the beginning of the MD simulation despite several unfavorable interactions between the LBD and MSVIII-19. As the MD simulations attempted to adjust KA2 around the bound MSVIII-19, however, the intramolecular hydrogen bond network of the receptor became unstable and disrupted. These simulations therefore suggest that the KA2 subunit cannot accommodate MSVIII-19 without either losing the key intermolecular interactions with the ligand or breaking the intramolecular structure of the LBD. It is also possible that other unfavorable interactions underlie the absence of MSVIII-19 binding; in any case, MD simulations did not reveal a plausible binding mode for the KA2 subunit.

Single Site Exchanges of Critical Residues in the GluR5 and KA2 Ligand Binding Domains. Modeling and MD simulations suggest that differences between GluR5 and KA2 at three critical binding site residues, Val685/Ile669, Leu735/Phe719, and Ser741/Met725, underlie the large divergence in binding affinity and functional activity. To test these predictions, we exchanged these residues in GluR5 and KA2 using single site-directed mutagenesis and measured the effect on binding affinity. A total of six single-site mutants were made initially: GluR5(V685I), GluR5(L735F), GluR5(S741M), KA2(I669V), KA2(F719L), and KA2(M725S). These mutants, as well as the wild-type GluR5 and KA2 subunits, were expressed in COS-7 cells and membrane preparations were isolated for radioligand binding and displacement assays. Saturation binding isotherms using [^{3}H]kainate were constructed for all of mutants to determine whether the mutations altered radioligand affinity, but the changes were relatively modest with the exception of GluR5(V685I), which had a 6-fold increased affinity, and KA2(F719L), with a 5-fold lower affinity (Table 1 and Fig. 2).

To determine the binding affinity of DH on the mutated receptors, we measured the displacement of [^{3}H]kainate by a range of concentrations of DH. IC_{50} values obtained from the

TABLE 1

K_d values for [^{3}H] kainate and K_i values for displacement of [^{3}H] kainate by DH and MSVIII-19 on kainate receptor mutants

K_d values were determined by fitting curves with one-site binding (hyperbola). K_d values are presented as mean ± S.E.M. K_i values were calculated using K_d values in Table with the Cheng-Prusoff equation ($K_i = IC_{50}/(1 + [\text{radioligand}]/K_d)$). K_i values are mean with 95% confidence intervals in parentheses. IC_{50} values were obtained using a one-site competition fit using Prism 4 software. Values are in nanomolar, except for bold values, which are micromolar.

	K_d [^{3}H]KA	K_i	
		DH	MSVIII-19
GluR5 WT	157 ± 35	3.1 (1.5–6.5)	100 (65–155)
V685I	25 ± 7.2*	6.1 (5.2–7.3)	**4.4 (3.0–6.3)**
L735F	145 ± 78	5.9 (4.3–8.2)	**1.2 (0.6–2.6)**
S741M	43 ± 11*	3.0 (1.9–4.9)	**2.6 (1.7–3.8)**
V685I/ S741M	15 ± 0.7*	4.8 (3.5–6.6)	**26 (15–46)**[a]
V685I/ L735F/ S741M	27 ± 2.2*	66 (38–116)	**72 (34–149)**[a]
KA2 WT	5.3 ± 4.1	**1.8 (1.3–2.4)**	**>100**
I669V	5.6 ± 0.5	18 (12–26)	**41 (26–65)**[a]
F719L	24 ± 9.9	81 (60–108)	**>100**
M725S	2.9 ± 0.6	5.2 (3.8–6.8)	**31 (23–42)**[a]
I669V/ M725S	12 ± 3.8	7.0 (5.5–8.8)	**4.0 (2.5–6.2)**
I669V/ F719L/ M725S	20 ± 4.2	29 (19–43)	**3.6 (2.6–5.1)**

* $P < 0.05$ based on unpaired, two-tail t-tests that compared K_d values for mutants and wild-type subunits.
[a] Values were estimated based on a partial fit with a one-site competition curve.

fitting of competition curves were then transformed to K_i values using the Cheng-Prusoff equation and the experimentally determined K_d values from the saturation isotherms. In control experiments, we determined K_i values for DH binding to GluR5 and KA2 of 3.1 nM and 1.8 μM, respectively (Table 1 and Fig. 2), which are somewhat higher (GluR5) and lower (KA2) than those determined previously but still considerably divergent (Sakai et al., 2001). Single site mutation of the GluR5 subunit did not result in significant changes in the affinity for DH (Fig. 2A, right); K_i values were determined to be 6.1, 5.9, and 3.0 nM for GluR5(V685I), GluR5(L735F), and GluR5(S741M), respectively (n = 3–6, Table 1). In contrast, mutation of each of the three residues in the KA2 subunit increased the affinity of DH (Fig. 2B, right). The K_i values for the displacement of [^{3}H]kainate from KA2(I669V), KA2(F719L), and KA2(M725S) were 18, 81, and 5.2 nM, respectively (n = 3–4, Table 1); notably, the latter has an affinity similar to that of wild-type GluR5 subunits (Fig. 2B, right). These results reveal a striking divergence in the effect of mutation of the LBD of these two KAR subunits on affinity for DH. GluR5 was relatively insensitive to introduction of an additional bulky group, whereas enlargement of the KA2 LBD with even a single site mutation greatly enhanced the affinity.

We next determined how mutation of these three residues altered MSVIII-19 binding to GluR5 and KA2 receptor subunits. Competitive displacement of [^{3}H] kainate produced K_i values of 100 nM for MSVIII-19 on GluR5 subunits (Table 1; Fig. 3A; n = 5) and >100 μM for KA2 subunits (Sanders et al., 2005). As shown in the displacement curves in Fig. 3A, mutation of any of the three residues in GluR5 resulted in a >10-fold reduction in affinity for MSVIII-19 (K_i values of 4.4, 1.2, and 2.6 μM for GluR5(V685I), GluR5(L735F), and GluR5(S741M), respectively, n = 3–5; also see Table 1). Conversely, the single residue mutations in the KA2 subunit increased affinity for MSVIII-19 from essentially no displacement in the wild-type to 41, 118, and 46 μM for KA2(I669V), KA2(F719L), and KA2(M725S), respectively (n = 3–5; Table 1 and Fig. 3B). These results support a critical role for hydrophobic residues that shape the dimensions of the LBD in determining affinity for the antagonist MSVIII-19.

Multiple Site Exchanges of Critical Residues in the GluR5 and KA2 Ligand Binding Domains. To determine whether addition of other bulky groups to the GluR5 LBD would affect binding affinity for DH or MSVIII-19, we generated double and triple site mutants of the three key residues. Binding affinities for kainate were increased for the GluR5 double and triple mutants as determined by saturation isotherms with [^{3}H]kainate (Table 1, Fig. 4). The double mutant GluR5(V685I/S741M) (also referred to as DM) had an affinity for DH similar to that of wild-type GluR5 (K_i = 4.8 nM, n = 4; Fig. 4A). However, the addition of three bulky side chains in the triple mutant, GluR5(V685I/L735F/S741M) (referred to as TM) resulted in a ~10-fold lower affinity for DH compared with the GluR5 subunit (K_i = 66 nM, n = 4; Fig. 4A). Thus, mutation of all three sites only partially reversed the high affinity and failed to recapitulate the very low affinity observed with wild-type KA2 subunits. Double and triple mutants of the KA2 subunit, KA2(I669V/M725S) and KA2(I669V/F719L/M725S), maintained the very high affinity observed with the single mutant (K_i values of 7.0 and 28.5 nM, respectively; n = 4–5, Fig. 4B), although the triple KA2 mutant exhibited a slightly lower affinity than either KA2(M725S) or KA2(I669V/M725S) subunits. In summary, reducing the number of bulky side chains in the KA2 LBD did not concomitantly increase affinity for DH.

Multiple site mutation of the GluR5 and KA2 LBDs had marked effects on the binding affinity of MSVIII-19. We observed only partial displacement of radioligand at the highest concentrations in the GluR5 DM and TM mutants, resulting in reductions in affinity of greater than 2 orders of magnitude to estimated K_i values of 26 and 72 μM, respectively (n = 5 and 4; Fig. 5A). Conversely, exchange of either both or all three of the residues in the KA2 subunit for the

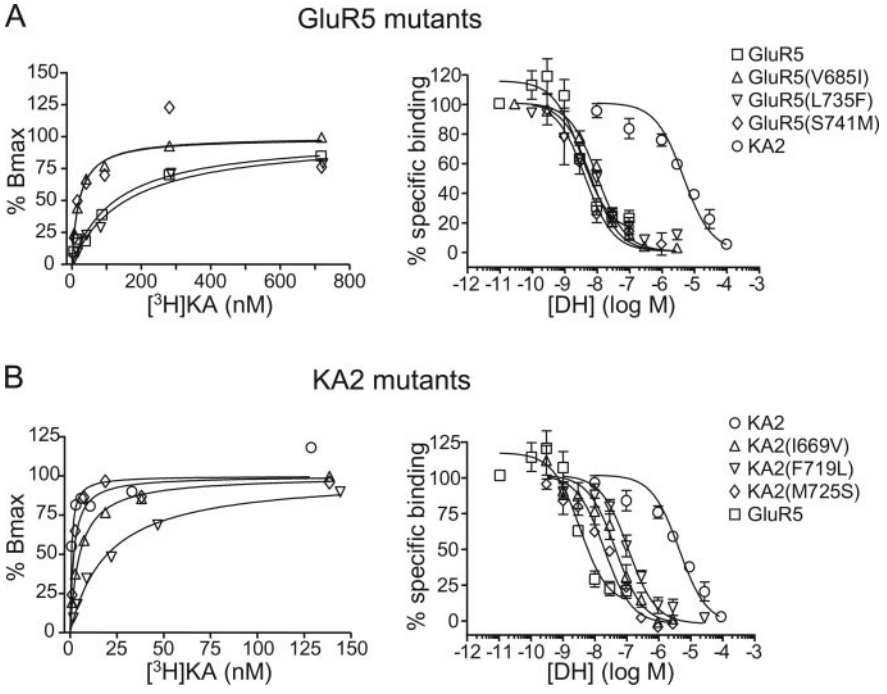

Fig. 2. Radioligand binding assays demonstrate that single site mutations reduce affinity of DH for KA2 subunits. A, saturation (left) and displacement experiments (right) were performed on GluR5(V685I) (△), (GluR5 L735F) (▽), GluR5(S741) (◇), GluR5 wildtype (□). B, saturation (left) and displacement experiments (right) were performed on KA2 wild-type (○), KA2(I669V) (△), KA2(F719L) (▽), KA2(M725S) (◇). Receptors expressed in COS-7 cells. [^{3}H]kainate was added at varying concentrations for saturation isotherms. Representative saturation curves are shown for each subunit, n = 3–4. Glutamate (1 mM) was used to determine nonspecific binding for saturation and displacement experiments. Saturation curves were fit with one-site binding (hyperbola) and displacement curves were fit with a one-site competition curve. n = 3–6 for each concentration of DH for displacement curves. K_d and K_i values obtained from these curves are found in Table 1.

corresponding residues in GluR5 resulted in a ~200-fold increase in the affinity for MSVIII-19 (K_i values of 4.0 and 3.6 μM, n = 4–5, respectively; Fig. 5B), which was a significant change but nevertheless not as high as wild-type GluR5 subunits. There was not a significant difference between the KA2 DM and TM mutants, suggesting that the I669V and M725S mutations are primarily responsible for the increase in affinity. This is in agreement with single KA2 mutants, wherein the I669V and M725S but not the F719L mutation resulted in increased MSVIII-19 affinity (Fig. 3B).

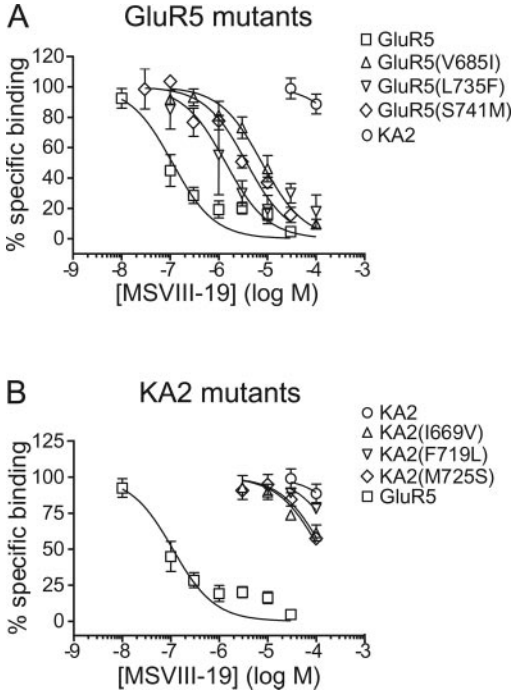

Fig. 3. Single site-mutations alter the affinity of MSVIII-19 on KA2 and GluR5 receptors. A, displacement of [^{3}H]kainate by MSVIII-19 on GluR5(V685I) (△), GluR5(L735F) (▽), GluR5(S741) (◇), and GluR5 wild type (□). B, displacement of [^{3}H]kainate by MSVIII-19 on KA2 wild type (○), KA2(I669V) (△), KA2(F719L) (▽), KA2(M725S) (◇). Receptors were expressed in COS-7 cells. KA2 wild-type binding data are shown for comparison and were taken from Sanders et al. (2005). Glutamate (1 mM) was used to determine nonspecific binding for saturation and displacement experiments. Displacement curves were fit with a one-site competition curve. n = 3–6 for each concentration of MSVIII-19 for displacement curves. K_i values calculated from these curves are found in Table 1.

Mutations That Alter Binding Affinity Affect the Physiological Activity of DH. To determine how the altered binding affinities manifested as changes in physiological action of DH, we carried out whole-cell recordings from human embryonic kidney 293 cells transfected with wild-type and mutant KARs. DH is a high-affinity agonist for homomeric GluR5 receptors that produces a long-lasting (>30 min) desensitization of GluR5 KARs after exposure to DH. To compare the duration of action of DH on wild-type and GluR5(TM) mutant receptors, which had the lowest binding affinity in displacement assays, we measured the recovery of glutamate-evoked responses after application of DH to these receptors. Figure 6A shows currents recorded from cells expressing GluR5 wild-type or GluR5(TM) receptors in response to glutamate (10 mM, left), DH (10 μM, center), and then glutamate 20 min (wild type) or 4 min (TM) after DH application. GluR5(TM) receptors were functional and exhibited variable rates of desensitization, similar to wild-type GluR5 receptors (Swanson and Heinemann, 1998). DH remained an agonist for GluR5(TM) despite the lower binding affinity. As shown in the figure, DH bound and desensitized wild-type GluR5 receptors, making them unavailable for subsequent activation by glutamate; this was not the case for GluR5(TM), which recovered quickly and produced glutamate-evoked currents within minutes after DH application. The rapid recovery time course is shown in Fig. 6B as the normalized peak current amplitude relative to the initial two-min preDH control amplitudes; GluR5(TM) recovered to near-control amplitudes with a time constant of

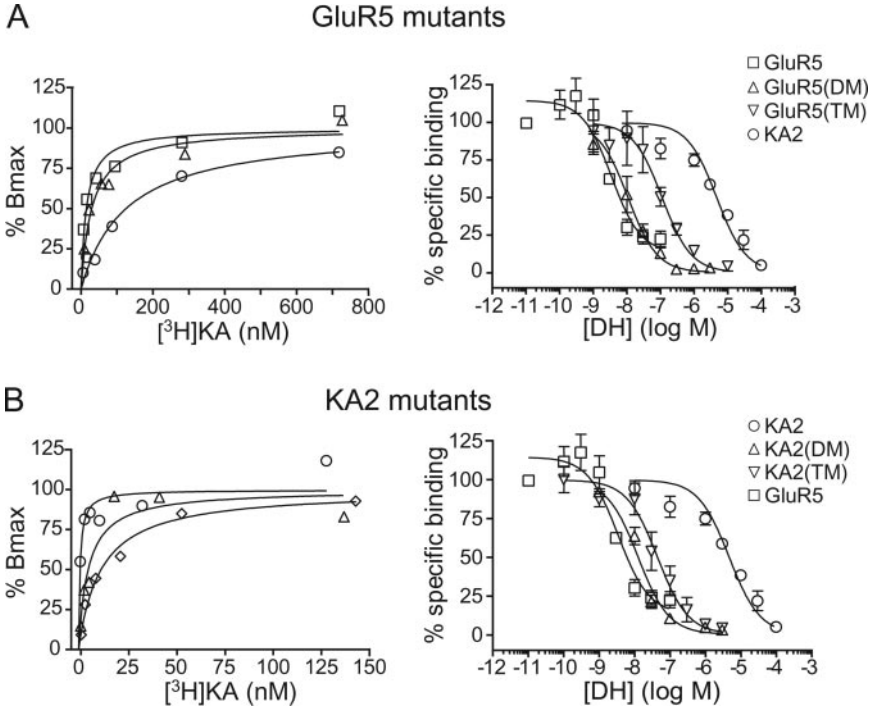

Fig. 4. Double and triple mutants decrease the affinity of DH for GluR5 subunits. A, saturation (left) and displacement (right) experiments were performed on GluR5(V685I/S741M) (DM) (△), GluR5(V685I/L735F/S741M) (TM) (▽), and GluR5 wild type (□). B, saturation (left) and displacement (right) experiments were performed on KA2 wildtype (○), KA2(I669V/M725S) (DM) (△), KA2(I669V/F719L/M725S) (TM) (▽). Receptors were expressed in COS-7 cells. [^{3}H]Kainate was added at varying concentrations for saturation isotherms. Representative saturation curves are shown for each subunit, n = 3–4. [^{3}H]Kainate was displaced by DH on KA2 (A, right) and GluR5 (B, right) wild-type and multiple mutants expressed in COS-7 cells. Glutamate (1 mM) was used to determine nonspecific binding for saturation and displacement experiments. Saturation curves were fit with one-site binding (hyperbola), and displacement curves were fit with a one-site competition curve. n = 3–6 for each concentration of DH for displacement curves. K_d and K_i values obtained from these curves are found in Table 1.

0.20 ± 0.02 min. For comparison, recovery data for GluR5 wild-type receptor currents after DH application are shown also (Swanson et al., 2002). In summary, the relatively fast recovery of GluR5(TM) receptors after application of DH is consistent with the lower affinity of DH for these mutated receptors.

To assess the effect of increasing the DH affinity for KA2 receptors in the KA2(DM) mutant, we recorded the responses elicited by glutamate and DH from heteromeric GluR5/KA2(DM) receptors. We showed previously that DH has an unusual activity on GluR5/KA2 receptors that arises from the highly divergent affinity for the two component subunits. In the presence of DH, GluR5/KA2 receptor currents activate and desensitize. However, after removal of DH from the bathing solution, a slowly activating steady-state current arises that has its genesis in the selective long-lasting activation of GluR5 subunits in the heteromeric receptor complex (whereas the KA2 subunit LBD remains unoccupied) (Swanson et al., 2002). Increasing the affinity of DH for KA2 should prevent the development of this steady-state current. This was indeed what we observed with the GluR5/KA2(DM) mutant, which was used because it had a higher affinity for DH than the triple mutant. As shown in Fig. 6C, glutamate (left) evoked desensitizing currents from heteromeric GluR5/KA2(DM) receptors that were similar in amplitude and kinetics to the GluR5/KA2 wild-type receptor. However, no steady-state current emerged after removal of DH, and subsequent applications of glutamate failed to elicit the typical "positive" jump back to baseline seen with GluR5/KA2 receptors (Fig. 6C). Instead, glutamate-evoked currents were attenuated for up to 20 min after application of DH (Fig. 6, C and D), similar to the long-lasting desensitized state observed with wild-type GluR5 homomeric receptors (Swanson et al., 2002). These data are consistent with the creation of high-affinity binding sites for DH in the KA2(DM) mutant, resulting in the functionally irreversible interaction with both GluR5 and KA2(DM) in the heteromeric receptor. In summary, the physiological data support the functional significance of the altered binding affinities for DH in the mutated GluR5 and KA2 subunits.

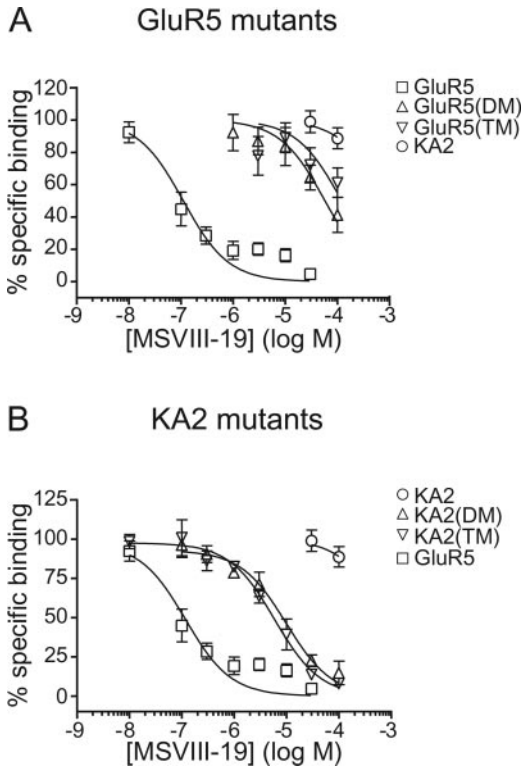

Fig. 5. Double and triple mutants alter the affinity of MSVIII-19 for KA2 and GluR5 subunits. A, [^{3}H]kainate was displaced by MSVIII-19 on GluR5(DM) (△), GluR5(TM) (▽), and GluR5 wild-type (□) receptors. B, [^{3}H]kainate was displaced by MSVIII-19 on KA2 wildtype (○), KA2(DM) (△), and KA2(TM) (▽) subunits. Receptors expressed in COS-7 cells. KA2 wild-type binding data are shown for comparison and were taken from Sanders et al., 2005. Glutamate (1 mM) was used to determine nonspecific binding for saturation and displacement experiments. Displacement curves were fit with a one-site competition curve. n = 3–6 for each concentration of MSVIII-19 for displacement curves. K_i values calculated from these curves are found in Table 1.

Ligand Binding Mutations Modify the Potency of MSVIII-19 As an Antagonist. MSVIII-19 is an AMPA and kainate receptor antagonist that inhibits homomeric GluR5 receptors with highest affinity (Sanders et al., 2005). Mutations that lower the affinity of MSVIII-19 for the GluR5 subunit should concomitantly result in a decreased sensitivity to inhibition by the compound. As seen in Fig. 7A, application of 10 μM MSVIII-19 inhibits activation of GluR5 wild-type receptors with glutamate almost completely, whereas GluR5(TM) receptors were inhibited by ~60%. The mean inhibition measured at a range of antagonist concentrations was fitted well with a single logistic relationship to derive an IC_{50} of 4.1 μM for GluR5(TM) receptors (Fig. 7B, n = 3), compared with an IC_{50} of 23 nM for wild-type GluR5 receptors (data shown in Fig. 7B taken from Sanders et al., 2005). Thus, a 720-fold reduction in binding affinity with the introduction of the three mutations into the GluR5 LBD was matched by a ~200-fold reduction in potency in functional experiments.

The concentration-inhibition curve for MSVIII-19 antagonism of heteromeric GluR5/KA2 receptor activation is very shallow, which is likely to arise from the divergent affinity of the compound for the two distinct component subunits. MSVIII-19 is also significantly less potent on these receptors compared with GluR5 receptors (IC_{50} of 1.9 μM). We next tested the effect of the KA2(DM) mutations, which increase the affinity for MSVIII-19, in whole-cell recordings from cells expressing GluR5/KA2(DM) receptors. Application of 10 μM MSVIII-19 inhibited wild-type GluR5/KA2 receptors by ~65% and GluR5/KA2(DM) receptors by ~86% in the representative recordings shown in Fig. 7C. We were surprised to find that IC_{50} values determined for GluR5/KA2 and GluR5/KA2(DM) were quite similar (1.9 and 1.4 μM, respectively, n = 3; Fig. 7D), but the fit to the GluR5/KA2(DM) data were clearly steeper than that of wild-type GluR5/KA2 receptors (Hill slopes of 1.0 versus 0.5, respectively). It is likely that the shallow inhibition curve observed from wild-type GluR5/KA2 receptors contains two components of divergent potency, consistent with the binding affinities for these subunits. Refitting of the dataset with two logistic components yielded IC_{50} values of 0.23 and 29 μM. The higher affinity of KA2(DM) subunits is much nearer to that of GluR5 receptors, which consequently manifests as a leftward shift of the low affinity inhibitory component and an increase in the Hill slope.

Discussion

The objective of this study was to identify the critical residues responsible for the divergent affinities of GluR5 and KA2 KAR subunits for the marine-derived compounds DH and MSVIII-19. These compounds are among the most selective ligands known to differentiate between KAR subunits, and MSVIII-19 represents a potentially useful lead in development of novel selective antagonists. Design of the next generation of synthetic DH-related molecules, which is the subject of ongoing research efforts, will be informed by an understanding of the key interactions between the ligands and receptor subunits.

Our modeling and simulations of the LBDs of GluR5 and KA2 suggested that three residues play a critical role in determining the selectivity of DH and MSVIII-19 and that binding of MSVIII-19 to GluR5 occurred principally through interactions with domain 1 of the LBD. Two of these three amino acids in GluR5, Val685 and Leu735, contain smaller hydrophobic side chains than their counterparts in KA2 and therefore contribute to shaping the relatively large dimensions of the GluR5 LBD compared with other iGluRs (Mayer, 2005; Naur et al., 2005). Conversely, modeling predicted that the bulkier side-chains at these positions in KA2 (Ile669 and Phe719) encroach upon key water molecules and force a rearrangement of the LBD that precludes interaction between the ligands and critical binding residues. Finally, our modeling predicted that the third divergent residue, Ser741, provides an opportunity for hydrogen bonding to the C8 sub-

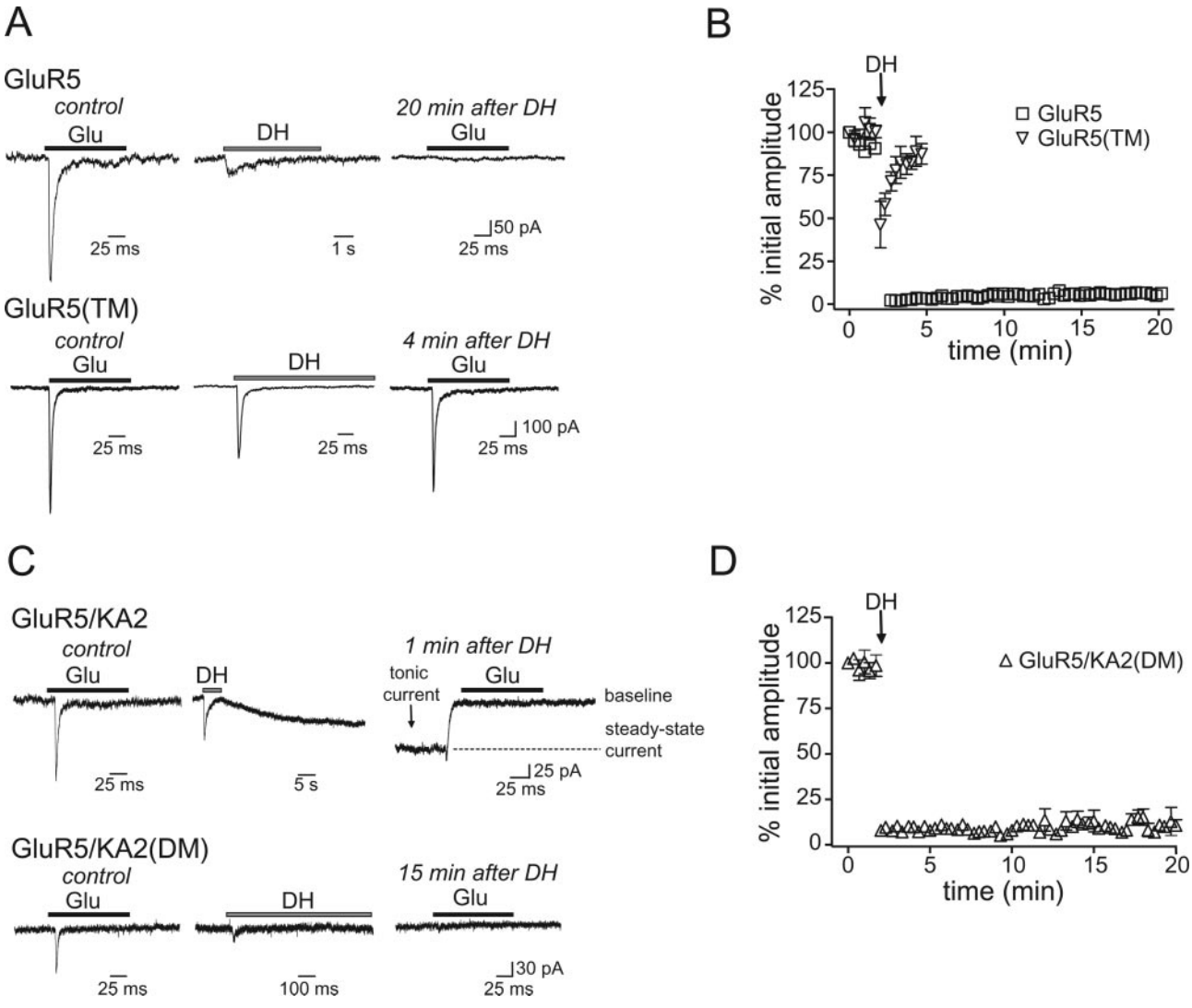

Fig. 6. DH displays a modified affinity for KA2 and GluR5 mutant receptors. A, representative traces showing the rate of recovery of glutamate (10 mM) responses evoked after the application of DH. The trace on the left represents a control response to 100-ms application of 10 mM glutamate. Middle trace shows the response of 5-s application of 10 μM DH. Right shows response evoked by 10 mM glutamate after 20 min for GluR5 and 4 min for GluR5(TM). B, comparison of rate of recovery of glutamate response for GluR5 (□) versus GluR5(TM) (▽). Amplitudes of currents evoked by glutamate were normalized to the first current response. Glutamate application occurred every 20 s. The data shown for the rate of recovery for the glutamate-evoked currents after DH application to GluR5 wild-type receptors was taken from our previous report for the sake of comparison (Swanson et al., 2002). C, application of DH to KA2(DM) receptors results in a long-lasting desensitized state. Representative traces are shown for response of DH on GluR5/KA2 (top) and GluR5/KA2(DM) (bottom). The trace on the left represents a response to 100-ms application of 10 mM glutamate. Middle trace shows the response of 5-s application of 10 μM DH. The right trace shows the response to glutamate immediately after DH application to wild-type GluR5/KA2 receptors or 15 min after DH application to GluR5/KA2(DM) receptors. D, amplitudes of the glutamate-evoked currents were normalized against the initial control response before application of DH to determine the kinetics of recovery after DH application. Glutamate applications occurred every 20 s. n = 3–4 for each time point.

stituent in DH that is not possible with Met725 in KA2. These residues were also identified as important determinants of the pharmacological specificity of the agonists ATPA and 5-iodowillardiine in docking models with the resolved structure of the GluR5 LBD (Mayer, 2005).

Structure-Function Studies with DH. Exchanging the critical residues between GluR5 and KA2 had a range of effects on binding affinity for DH. The most striking result was the creation of a high-affinity binding site for DH with single mutations of the KA2 subunit LBD. In particular, the mutation KA2(M725S) increased the affinity for DH by ~350-fold; DH affinity for KA2(I669V) and KA2(F719L) were also ~100- and 22-fold higher, respectively. Combining mutations in KA2(DM) did not further increase the affinity for DH beyond that observed for KA2(M725S). In fact, the triple mutant KA2(TM) had a reduced affinity compared with KA2(M725S) or KA2(DM) receptors. The KA2(DM) receptor exhibited physiological behavior consistent with the presence of a high-affinity binding site for DH; that is, application of the compound to GluR5/KA2(DM) replicated the long-lasting agonist-bound and desensitized state observed with homomeric GluR5 receptors. The patch-clamp recordings also provide further support for our hypothesis that the slowly activating tonic current that arises after DH application to GluR5/KA2 receptors (see Fig. 6) predominantly reflects kinetics of DH interaction with the KA2 subunit (Swanson et al., 2002). These results demonstrate that multiple residues in the KA2 LBD effectively occlude binding of DH. Relief of steric hindrance or formation of a hydrogen bond with the Ser725 hydroxyl group greatly increased affinity consistent

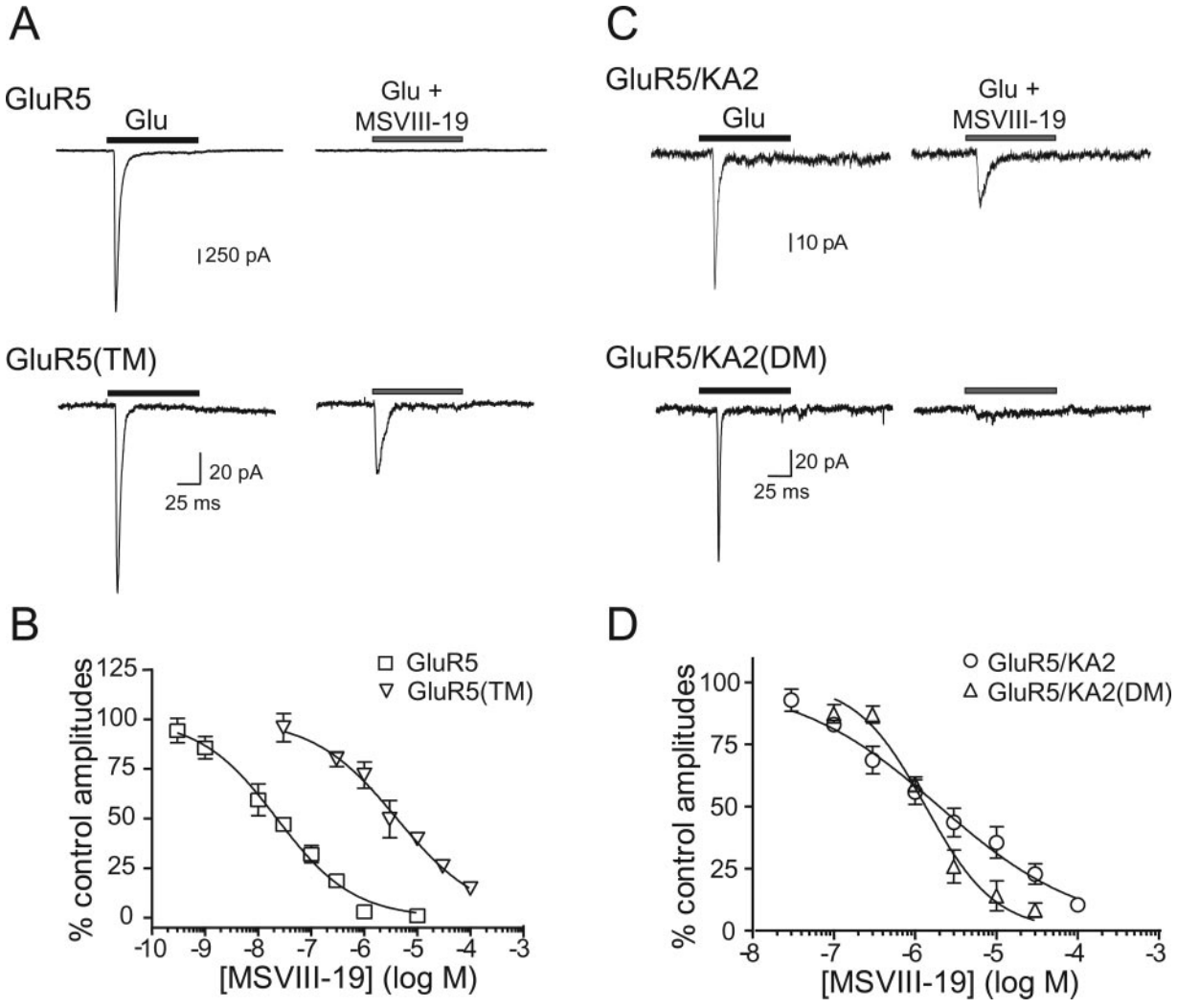

Fig. 7. Inhibition by MSVIII-19 of KA2 and GluR5 receptors is altered by mutations. A, representative currents traces showing inhibition by 10 μM MSVIII-19 on GluR5 (top) and GluR5(TM) (bottom). The traces on the left show control responses evoked by 100-ms application of 10 mM glutamate (black bars). Traces on the right show responses to coapplication of 10 μM MSVIII-19 and 10 mM glutamate (gray bars). GluR5 wild-type traces are modified from Sanders et al. (2005) and are shown for comparative purposes. B, concentration-inhibition curves for MSVIII-19 on GluR5 (□) and GluR5(TM) (▽). The GluR5 concentration-inhibition curve is taken from previous data (Sanders et al., 2005). IC_{50} values are 23 nM and 4.1 μM on GluR5 (Sanders et al., 2005) and GluR5(TM) (n = 3–5 for each MSVIII-19 concentration). Curves were generated with a sigmoidal dose-response (variable slope) curve. C, comparison of inhibition by 10 μM MSVIII-19 on glutamate evoked responses from GluR5/KA2 (top) and GluR5/KA2(DM) (bottom). Traces on left represent control responses evoked by 100-ms application of 10 mM glutamate (black bars). On the right, traces show the amount of inhibition by 10 μM MSVIII-19 when coapplied with 10 mM glutamate (gray bars). For comparison, representative traces were modified from previous data (Sanders et al., 2005). D, concentration-inhibition curves for MSVIII-19 on GluR5/KA2 (○) and GluR5/KA2(DM) (△). Concentration-inhibition curve for GluR5/KA2 wildtype was taken from Sanders et al., 2005. IC_{50} values of 1.9 μM and 1.4 μM were obtained for GluR5/KA2 (Sanders et al., 2005) and GluR5/KA2(DM) (n = 3–4 for each concentration of MSVIII-19). Curves were generated with a sigmoidal dose-response (variable slope) curve.

with the predictions of our model and those made previously on the basis of docking models (Mayer, 2005). As well, the equivalent DH affinity and functional behavior observed for GluR5 (wild type) and the KA2(DM) mutant suggest that the LBDs of these distinct subunits assume similar conformations, at least in the presence of DH.

In contrast to the large effects observed with mutation of the KA2 subunit, reciprocal single mutations in the GluR5 subunit resulted in relatively little change in affinity for DH. This surprising result was not predicted by the models, which suggested that introduction of steric hindrance or elimination of the Ser741 hydroxyl group would profoundly alter DH affinity. It is possible that the relatively large binding cavity of GluR5 subunits marginalizes the introduction of individual bulky groups or that the LBD is more flexible than can be accounted for in modeling or simulations. The unchanged affinity of the S741M mutation, in particular, was unexpected because we predicted the serine hydroxyl group would form a hydrogen bond with the C8 functional group in DH and neo-DH, a natural analog containing a hydroxyl rather than a methylamine C8 moiety. Neo-DH displays ~10-fold lower affinity for GluR5 subunits, which we attributed previously to a reduction in the number of potential hydrogen bonds formed from two [with the methylamine group of DH (to Glu738 and Ser741)] to one [with the hydroxyl group of neoDH (to Ser741)]. It should be noted that the methionine-containing structure shown in Fig. 1B would certainly result in steric hindrance, suggesting the conformation shown in the image is unlikely to be correct and that the methionine side-chain exists in an alternate conformation (or that larger scale accommodations occur in the GluR5(S741M) mutant). On the other hand, the residue at Ser741 (Met725 in KA2) might affect ligand affinity primarily through influences on the relative distance between the C9 hydroxyl moiety in DH (and neo-DH) and Glu738, because our preliminary results suggest this site is a particularly critical determinant of KAR affinity (J. M. Sanders and G. T. Swanson, unpublished results). Introduction of three bulky residues in GluR5(TM) subunits only shifted the affinity for DH by ~20-fold despite nearly recapitulating the local sequence differences in the LBD between GluR5 and KA2, which underscores the limitations in static models or simulations of these dynamic structures. Until crystal structures are resolved, however, functional studies, mutagenesis and model-building remain the most accessible strategy for understanding the molecular pharmacology of these compounds.

Structure-Function Studies with MSVIII-19. We predict that MSVIII-19 exhibits antagonist activity on GluR5 primarily because this molecule does not stabilize the lobe rotation, or closure, thought to be critical for channel activation of non-NMDA receptors. The C8 and C9 functional groups that, in DH, stabilize the high-affinity interactions with GluR5 and GluR6 receptors are absent and are likely to be replaced by water molecules. This mechanism of action is distinct from that of antagonists that have been resolved in complex with GluR2 [6,7-dinitro-2,3-quinoxalinedione, (*S*)-2-amino-3-[5-tert-butyl-3-(phosphonomethoxy)-4-isoxazolyl] propionic acid] or the NR1 NMDA receptor (dichlorokynurenic acid, cycloleucine) LBDs (Armstrong and Gouaux, 2000; Furukawa and Gouaux, 2003; Hogner et al., 2003; Inanobe et al., 2005). These antagonists prevent interdomain interactions through direct binding of critical residues or by steric hindrance. In contrast to DH, which retains a low affinity for KA2 subunits, MSVIII-19 has no apparent affinity for KA2 subunits. We hypothesize that the absence of the C9 hydroxyl group, which probably forms a critical hydrogen bond with the main chain amino group of Glu738, renders MSVIII-19 susceptible to unfavorable steric hindrance from the bulkier amino acids in KA2. On the other hand, the larger side-chains in KA2 might affect the positioning of water molecules and secondarily the affinity of MSVIII-19. Introduction of even one bulky side chain in the single GluR5 mutants markedly reduced the MSVIII-19 affinity by 10- to 45-fold, and the GluR5(TM) triple mutant was of ~700-fold lower affinity. Based on the simulation shown in Fig. 1D, the V685I and L735F mutations affect the positions of waters w1 and w2, thereby altering hydrogen bonding to the γ-carboxyl group as well as the tetrahydropyran oxygen. Introduction of a methionine side-chain into Ser741 of GluR5 distorts the structure of the binding pocket in MD simulations. Relief of these unfavorable interactions in the KA2 mutants conversely resulted in increased affinity for MSVIII-19, with the exception of KA2(F719L). Introduction of two or three mutations in KA2 greatly increased affinity to only ~10-fold less than that observed with GluR5, which was partly reflected in an increased sensitivity to inhibition in physiological assays.

These results demonstrate that the determinants in the GluR5 and KA2 LBDs that confer specificity for particular kainate receptor subunits largely overlap for DH and MSVIII-19. Not surprisingly, these same residues are probably central to the binding and selectivity of other kainate (and AMPA) receptor ligands. For example, ATPA, a GluR5 selective agonist, was predicted to form a complex via a water molecule with Ser741; mutation of this residue to methionine resulted in a decreased affinity for ATPA (Nielsen et al., 2003). An equivalent site mutant markedly reduced the affinity of GluR5 for MSVIII-19 in our experiments. These data and our current study support the permissive role of the serine residue in the selective binding of ligands to the GluR5 LBD.

In summary, the selective binding of DH and MSVIII-19 to KARs depends on interactions with three residues residing in the S2 portion of the LBD. We show that changing these residues in the KA2 subunit significantly increases the binding affinity of the ligands. Reciprocal mutations in the GluR5 subunit result in only a modest decrease in DH affinity, whereas they result in a sizeable decrease in MSVIII-19 affinity. These data provide experimental support for both modeling and structural data. Synthesis of this information with other mutagenesis, modeling, and structural data will facilitate the design and pharmacological characterization of novel, subunit-selective compounds for the various subtypes of KARs, which will be of use toward understanding the spectrum of physiological and pathophysiological actions of KARs in the CNS.

Acknowledgments

We thank the Centre for Scientific Computing (CSC, Espoo, Finland) for access to the docking software.

References

Armstrong N and Gouaux E (2000) Mechanisms for activation and antagonism of an AMPA-sensitive glutamate receptor: crystal structures of the GluR2 ligand binding core. *Neuron* **28:**165–181.

Barton ME, Peters SC, and Shannon HE (2003) Comparison of the effect of gluta-

mate receptor modulators in the 6 Hz and maximal electroshock seizure models. *Epilepsy Res* **56:**17–26.
Bayly CI, Cieplak P, Cornell WD, and Kollman PA (1993) A well-behaved electrostatic potential based method using charge restraints for deriving atomic charges: the RESP model. *J Phys Chem* **97:**10269–10280.
Case DA, Cheatham TE 3rd, Darden T, Gohlke H, Luo R, Merz KM Jr, Onufriev A, Simmerling C, Wang B, and Woods RJ (2005) Amber biomolecular simulation programs. *J Computat Chem* **26:**1668–1688.
Christensen JK, Varming T, Ahring PK, Jorgensen TD, and Nielsen EO (2004) In vitro characterization of 5-carboxyl-2,4-di-benzamidobenzoic acid (NS3763), a non-competitive antagonist of GLUK5 Receptors. *J Pharmacol Exp Ther* **309:**1003–1010.
Cieplak P, Cornell WD, Bayly C, and Kollman PA (1995) Application of the multimolecule and multiconformational RESP methodology to biopolymers: charge derivation for DNA, RNA and proteins. *J Comput Chem* **16:**1357–1377.
Cornell WD, Cieplak P, Bayly CI, and Kollman PA (1993) Application of RESP charges to calculate conformational energies, hydrogen bond energies and free energies of solvation. *J Am Chem Soc* **115:**9620–9631.
Darden T, York D, and Pedersen L (1993) Particle mesh Ewald: an N·log(N) method for Ewald sums in large systems. *J Chem Phys* **98:**10089–10092.
Dingledine R, Borges K, Bowie D, and Traynelis SF (1999) The glutamate receptor ion channels. *Pharmacol Rev* **51:**7–62.
Essmann U, Perera L, Berkowitz ML, Darden T, Lee H, and Pedersen LG (1995) A smooth particle mesh Ewald method. *J Chem Phys* **103:**8577–8593.
Frisch MJ, Trucks GW, Schlegel HB, Scuseria GE, Robb MA, Cheeseman JR, Montgomery JA Jr, Vreven T, Kudin KN, Burant JC, et al. (2004) Gaussian 03, Gaussian, Inc., Wallingford CT.
Furukawa H and Gouaux E (2003) Mechanisms of activation, inhibition and specificity: crystal structures of the NMDA receptor NR1 ligand-binding core. *EMBO (Eur Mol Biol Organ) J* **22:**2873–2885.
Gilron I, Max MB, Lee G, Booher SL, Sang CN, Chappell AS, and Dionne RA (2000) Effects of the 2-amino-3-hydroxy-5-methyl-4-isoxazole-proprionic acid/kainate antagonist LY293558 on spontaneous and evoked postoperative pain. *Clin Pharmacol Ther* **68:**320–327.
Hogner A, Greenwood JR, Liljefors T, Lunn ML, Egebjerg J, Larsen IK, Gouaux E, and Kastrup JS (2003) Competitive antagonism of AMPA receptors by ligands of different classes: crystal structure of ATPO bound to the GluR2 ligand-binding core, in comparison with DNQX. *J Med Chem* **46:**214–221.
Hollmann M and Heinemann S (1994) Cloned glutamate receptors. *Annu Rev Neurosci* **17:**31–108.
Inanobe A, Furukawa H, and Gouaux E (2005) Mechanism of partial agonist action at the NR1 subunit of NMDA receptors. *Neuron* **47:**71–84.
Jin R, Banke TG, Mayer ML, Traynelis SF, and Gouaux E (2003) Structural basis for partial agonist action at ionotropic glutamate receptors. *Nat Neurosci* **6:**803–810.
Johnson MS and Overington JP (1993) A structural basis for sequence comparisons. An evaluation of scoring methodologies. *J Mol Biol* **233:**716–738.
Jones G, Willett P, and Glen RC (1995) Molecular recognition of receptor sites using a genetic algorithm with a description of desolvation. *J Mol Biol* **245:**43–53.
Jones G, Willett P, Glen RC, Leach AR, and Taylor R (1997) Development and validation of a genetic algorithm for flexible docking. *J Mol Biol* **267:**727–748.
Kew JN and Kemp JA (2005) Ionotropic and metabotropic glutamate receptor structure and pharmacology. *Psychopharmacology (Berl)* **179:**4–29.
Kraulis J (1991) MOLSCRIPT: A program to produce both detailed and schematic plots of protein structures. *J Appl Crystallogr* **24:**946–950.
Lehtonen JV, Still DJ, Rantanen VV, Ekholm J, Bjorklund D, Iftikhar Z, Huhtala M, Repo S, Jussila A, Jaakkola J, et al. (2004) BODIL: a molecular modeling environment for structure-function analysis and drug design. *J Comput Aided Mol Des* **18:**401–419.
Lovell SC, Word JM, Richardson JS, and Richardson DC (2000) The penultimate rotamer library. *Proteins* **40:**389–408.
Mayer ML (2005) Crystal structures of the GluR5 and GluR6 ligand binding cores: molecular mechanisms underlying kainate receptor selectivity. *Neuron* **45:**539–552.
Merritt E and Bacon D (1997) Raster3D: photorealistic molecular graphics. *Methods Enzymol* **277:**505–524.
More JC, Nistico R, Dolman NP, Clarke VR, Alt AJ, Ogden AM, Buelens FP, Troop HM, Kelland EE, Pilato F, et al. (2004) Characterisation of UBP296: a novel, potent and selective kainate receptor antagonist. *Neuropharmacology* **47:**46–64.
Nanao MH, Green T, Stern-Bach Y, Heinemann SF, and Choe S (2005) Structure of the kainate receptor subunit GluR6 agonist-binding domain complexed with domoic acid. *Proc Natl Acad Sci USA* **102:**1708–1713.
Naur P, Vestergaard B, Skov LK, Egebjerg J, Gajhede M, and Kastrup JS (2005) Crystal structure of the kainate receptor GluR5 ligand-binding core in complex with (*S*)-glutamate. *FEBS Lett* **579:**1154–1160.
Nielsen MM, Liljefors T, Krogsgaard-Larsen P, and Egebjerg J (2003) The selective activation of the glutamate receptor GluR5 by ATPA is controlled by serine 741. *Mol Pharmacol* **63:**19–25.
Oh BH, Ames GF, and Kim SH (1994) Structural basis for multiple ligand specificity of the periplasmic lysine-, arginine-, ornithine-binding protein. *J Biol Chem* **269:**26323–26330.
Pentikäinen U, Settimo L, Johnson MS, and Pentikäinen OT (2006) Subtype selectivity and flexibility of ionotropic glutamate receptors upon ligand binding. *Org Biomol Chem* **4:**1058–1070.
Ryckaert JP, Ciccotti G, and Berendsen HJC (1977) Numerical integration of the cartesian equations of motion of a system with constraints: molecular dynamics of *n*-alkanes. *J Comput Phys* **23:**327–341.
Sagui C and Darden TA (1999) *Simulation and Theory of Electrostatic Interactions in Solution.* American Institute of Physics, Melville, New York.
Sakai R, Kamiya H, Murata M, and Shimamoto K (1997) Dysiherbaine: a new neurotoxic amino acid from the Micronesian marine sponge *Dysidea herbacea. J Am Chem Soc* **119:**4112–4116.
Sakai R, Swanson GT, Shimamoto K, Green T, Contractor A, Ghetti A, Tamura-Horikawa Y, Oiwa C, and Kamiya H (2001) Pharmacological properties of the potent epileptogenic amino acid dysiherbaine, a novel glutamate receptor agonist isolated from the marine sponge *Dysidea herbacea*. *J Pharmacol Exp Ther* **296:**650–658.
Sanders JM, Ito K, Settimo L, Pentikainen OT, Shoji M, Sasaki M, Johnson MS, Sakai R, and Swanson GT (2005) Divergent pharmacological activity of novel marine-derived excitatory amino acids on glutamate receptors. *J Pharmacol Exp Ther* **314:**1068–1078.
Sang CN, Hostetter MP, Gracely RH, Chappell AS, Schoepp DD, Lee G, Whitcup S, Caruso R, and Max MB (1998) AMPA/kainate antagonist LY293558 reduces capsaicin-evoked hyperalgesia but not pain in normal skin in humans. *Anesthesiology* **89:**1060–1067.
Sang CN, Ramadan NM, Wallihan RG, Chappell AS, Freitag FG, Smith TR, Silberstein SD, Johnson KW, Phebus LA, Bleakman D, et al. (2004) LY293558, a novel AMPA/GluR5 antagonist, is efficacious and well-tolerated in acute migraine. *Cephalalgia* **24:**596–602.
Sasaki M, Maruyama T, Sakai R, and Tachibana K (1999) Synthesis and biological activity of dysiherbaine model compound. *Tetrahedron Lett* **40:**3195–3198.
Schafmeister CEAF, Ross WS, and Romanovski V (1995) LEaP, University of California, San Francisco.
Stern-Bach Y, Bettler B, Hartley M, Sheppard PO, O'Hara PJ, and Heinemann SF (1994) Agonist selectivity of glutamate receptors is specified by two domains structurally related to bacterial amino acid-binding proteins. *Neuron* **13:**1345–1357.
Swanson GT, Green T, Sakai R, Contractor A, Che W, Kamiya H, and Heinemann SF (2002) Differential activation of individual subunits in heteromeric kainate receptors. *Neuron* **34:**589–598.
Swanson GT and Heinemann SF (1998) Heterogeneity of homomeric GluR5 kainate receptor desensitization expressed in HEK293 cells. *J Physiol (Lond)* **513:**639–646.
Wang J, Wolf RM, Caldwell JW, Kollman PA, and Case DA (2004) Development and testing of a general amber force field. *J Comput Chem* **25:**1157–1174.
Word JM, Lovell SC, Richardson JS, and Richardson DC (1999) Asparagine and glutamine: using hydrogen atom contacts in the choice of side-chain amide orientation. *J Mol Biol* **285:**1735–1747.

Address correspondence to: Dr. Geoffrey T. Swanson, Department of Molecular Pharmacology and Biological Chemistry, Northwestern University Feinberg School of Medicine, Searle 7-443, 303 E. Chicago Avenue, Chicago, IL 60611. E-mail: gtswanson@northwestern.edu.